Biophysical Chemistry 149 (2010) 34–39

Contents lists available at ScienceDirect

Biophysical Chemistry

journal homepage: http://www.elsevier.com/locate/biophyschem

Binding affinity and mode of distamycin A with A/T stretches in double-stranded DNA: Importance of the terminal A/T residues

Mariko Asagi, Akira Toyama [1], Hideo Takeuchi *

Graduate School of Pharmaceutical Sciences, Tohoku University, Aobayama, Sendai 980-8578, Japan

ARTICLE INFO

Article history:
Received 16 February 2010
Accepted 19 March 2010
Available online 27 March 2010

Keywords:
Distamycin A
DNA
Circular dichroism
Binding mode
Singular value decomposition

ABSTRACT

Distamycin A (Dst) is an antibiotic which binds to the minor groove of double-stranded DNA at A/T-rich regions. We have examined the affinity and mode of Dst binding to DNA duplexes containing a conserved A/T core and variable terminal A/T regions by using circular dichroism spectroscopy. The observed circular dichroism spectra were analyzed by singular value decomposition and fitted to a two-step binding model. The result clearly shows a correlation between the affinity for Dst and the preference for Dst–DNA 1:1 binding over 2:1 binding. The A/T stretches that prefer 1:1 binding form high-affinity 1:1 complexes, whereas those preferring 2:1 binding form stable 2:1 complex with low overall affinities. The terminal A/T residues of the Dst binding region play an important role in the stabilization/destabilization of the 1:1 and 2:1 complexes, resulting in a terminal residue-dependent variation of the binding affinity and the binding mode preference.

1. Introduction

Distamycin A (Dst) is an antibiotic produced by the bacterium *Streptomyces distallicus*. The chemical structure of Dst is characterized by a chain of three *N*-methylpyrrole rings interconnected through a planar amide group and terminated with neutral formamide and positively charged propylamidinium (Fig. 1A) [1]. Since the discovery of a possible link between the antibiotic activity of Dst and its binding to double-stranded DNA [2], the interaction of Dst with DNA has been studied extensively, mostly from the standpoint of possible use of the DNA binder as a lead compound for developing new antitumor agents [3–5].

Footprinting binding assays have shown that Dst prefers A/T residues to G/C and binds to A/T-rich stretches of four or more base pairs [6–11]. Structural analyses by X-ray crystallography and solution nuclear magnetic resonance (NMR) have revealed that there are two types of Dst–DNA complexes, 1:1 and 2:1, whose occurrence depends on the DNA base sequence [12–19]. In the 1:1 complex, a Dst molecule fits into the DNA minor groove with the molecular backbone extending along the groove trough (Fig. 1B) [12,13], while, in the 2:1 complex, a widened minor groove accommodates two Dst molecules stacked side-by-side in a head-to-tail (antiparallel) orientation (Fig. 1C) [14–19]. In both complexes, the adenine N3 and thymine O2 atoms are recognized by Dst through amide NH hydrogen bonding. Circular dichroism (CD) and calorimetric studies have provided binding constants of 1:1 and 2:1 complexes of Dst with some DNA oligomers [20–23]. Despite the extensive studies on the Dst–DNA binding, it is still unclear what governs the binding affinity and mode.

A systematic study on the base sequence dependence of the Dst binding affinity was performed by Boger et al. [24], who applied a fluorescent intercalator displacement method to a library of 512 DNA hairpins containing all possible combinations of A, T, G, and C at five consecutive residue sites within the double-stranded hairpin stem. According to that study, the five-residue sequence most preferred by Dst is 5′-ATAAT-3′. The assay data of Boger et al. have further revealed that replacement of even one base on the 5′-or 3′-end of the ATAAT sequence significantly reduces the binding affinity, implying the importance of terminal residues in the Dst–DNA interaction.

In this study, we have investigated the effect of terminal residues on the affinity and mode of Dst binding by using CD spectroscopy, which provides clear distinction between the 1:1 and 2:1 complexes [20–23]. The most preferred pentamer sequence ATAAT and its 5′- and/or 3′-terminal variants (ATAA<u>A</u>, <u>T</u>TAAT, and <u>T</u>TAA<u>A</u>; substituted bases are underlined) were used for the investigation of terminal residue effect. Effects of addition of A/T or G/C residues to each end of 5′ and 3′ of ATAAT were also examined by using seven oligomers containing the following A/T stretches: <u>A</u>ATAAT<u>A</u>, <u>A</u>ATAAT<u>T</u>, <u>T</u>ATAAT<u>A</u>, <u>T</u>ATAAT<u>T</u>, ATAAT<u>AT</u>, <u>C</u>ATAAT<u>C</u>, and <u>C</u>ATAAT<u>G</u> (double underlined residues were added). The results clearly show that the terminal A/T residues of the Dst binding region affect the affinity for Dst as well as the preference for 1:1 or 2:1 binding.

* Corresponding author. Tel./fax: +81 22 795 6855.
E-mail address: takeuchi@mail.tains.tohoku.ac.jp (H. Takeuchi).
[1] Present address: Medical and Dental Hospital, Niigata University, 1-754 Asahimachi-dori, Niigata 951-8520, Japan.

0301-4622/$ – see front matter © 2010 Elsevier B.V. All rights reserved.
doi:10.1016/j.bpc.2010.03.014

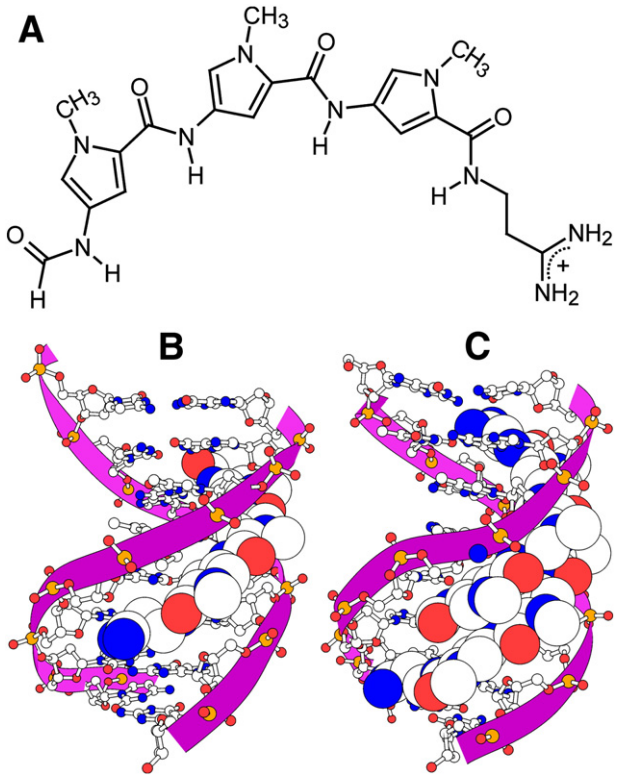

Fig. 1. Structure of distamycin A (Dst) and its binding to DNA. (A) Chemical structure of Dst. (B) Structure of a 1:1 Dst–DNA complex. (C) Structure of a 2:1 Dst–DNA complex. Dst is represented as a space-filling model in (B) and (C). The atomic coordinates of the 1:1 and 2:1 complexes are taken from Protein Data Bank (codes 1JTL and 378D) [13,18].

ATAAT	5'-GGC**ATAAT**CGC-3' 3'-CCG**TATTA**GCG-5'
ATAA<u>A</u>	5'-GGC**ATAAA**CGC-3' 3'-CCG**TATTT**GCG-5'
<u>T</u>TAAT	5'-GGC**TTAAT**CGC-3' 3'-CCG**AATTA**GCG-5'
<u>T</u>TAA<u>A</u>	5'-GGC**TTAAA**CGC-3' 3'-CCG**AATTT**GCG-5'
<u>A</u>ATAAT<u>A</u>	5'-GGC**AATAATA**CGC-3' 3'-CCG**TTATTAT**GCG-5'
<u>A</u>ATAAT<u>T</u>	5'-GGC**AATAATT**CGC-3' 3'-CCG**TTATTAA**GCG-5'
<u>T</u>ATAAT<u>A</u>	5'-GGC**TATAATA**CGC-3' 3'-CCG**ATATTAT**GCG-5'
<u>T</u>ATAAT<u>T</u>	5'-GGC**TATAATT**CGC-3' 3'-CCG**ATATTAA**GCG-5'
ATAAT<u>AT</u>	5'-GGC**ATAATAT**CGC-3' 3'-CCG**TATTATA**GCG-5'
<u>C</u>ATAAT<u>C</u>	5'-GGC**CATAATC**CGC-3' 3'-CCG**GTATTAG**GCG-5'
<u>G</u>ATAAT<u>C</u>	5'-GGC**GATAATC**CGC-3' 3'-CCG**CTATTAG**GCG-5'

Fig. 2. Deoxyoligonucleotides used in this study and their names. The single and double underlined bases were, respectively, substituted in and added to the sequence ATAAT.

2. Materials and methods

2.1. Materials

Deoxyoligonucleotides of the sequence 5′-GGC$(X)_n$CGC-3′ (X represents A, T, G, or C and *n* is 5 or 7) and its complimentary sequence were purchased from ESPEC Oligo Service. The terminal 5′-GGC and CGC-3′ triplets were added to achieve the following two purposes: (a) to reinforce the duplex formation between complimentary oligonucleotides by using strong G·C base-pairing and (b) to avoid self-complementarity that might lead to the formation of single-stranded hairpins. The DNA oligomers purchased were purified by reversed-phase HPLC on a $5C_{18}$-AR column (Nacalai Tesque) using an ammonium acetate–acetonitrile buffer system. After lyophilization, the dried DNA was dissolved in 0.1 M Tris–HCl buffer (pH 7.0) supplemented with 0.2 M NaCl, and then the solution was subjected to gel filtration on an NAP-25 column (Pharmacia). The concentration of DNA was determined from the absorbance at 260 nm at room temperature. The molar extinction coefficient (ε_{260}) of each DNA oligomer was first calculated from those of the component nucleotides assuming an unfolded structure [25] and then multiplied by a factor to correct any folding effect of the single-stranded oligomer at room temperature. The correction factor for ε_{260} was in a range of 0.94–0.98 as determined from the ratio of absorbance at room temperature (22–24 °C) to that at 80 °C (70 °C for short oligomers), where the oligomer was expected to be fully unfolded.

Double-stranded DNA oligomers were prepared by mixing mutually complimentary oligonucleotides at a 1:1 molar ratio. To ascertain the formation of duplexes, the absorption intensity at 260 nm was measured as a function of temperature. The observed UV melting curves showed clear transitions at 50.8–61.4 °C, indicating essentially complete duplex formation at room temperature. The DNA duplexes used in this study are listed in Fig. 2 together with their abbreviated names.

Powder samples of Dst hydrochloride were purchased from Sigma and dissolved in the same buffer as employed for preparing DNA solutions (0.1 M Tris–HCl, pH 7.0, 0.2 M NaCl). The concentration of Dst was determined by using a molar extinction coefficient of 34,000 M^{-1} cm^{-1} at 303 nm [26].

2.2. Spectral measurement

Solution samples for UV absorption and CD measurements were prepared by mixing Dst and DNA solutions to final concentrations of 0–20 μM (13 or 12 different concentrations) for Dst and 5 μM for DNA. The mixture solution was incubated at 37 °C for 24 h to ensure equilibration. UV absorption and CD spectra were recorded at room temperature on a Hitachi U-3310 spectrophotometer and a JASCO J-820 (or J-720) spectropolarimeter, respectively, using a quartz cell of 10 mm path length.

2.3. Spectral data analysis

The binding of Dst to DNA was analyzed using a simple two-step binding model:

$$2\mathrm{Dst} + \mathrm{DNA} \leftrightarrow \mathrm{Dst} + \mathrm{Dst}\cdot\mathrm{DNA} \leftrightarrow \mathrm{Dst}_2\cdot\mathrm{DNA} \quad (1)$$

where Dst·DNA and Dst_2·DNA stand for the 1:1 and 2:1 complexes of Dst and DNA, respectively. The first and second binding constants K_1 and K_2 are defined as follows:

$$K_1 = [\mathrm{Dst}\cdot\mathrm{DNA}] / [\mathrm{Dst}][\mathrm{DNA}] \quad (2)$$

$$K_2 = [\mathrm{Dst}_2\cdot\mathrm{DNA}] / [\mathrm{Dst}][\mathrm{Dst}\cdot\mathrm{DNA}] \quad (3)$$

For each DNA duplex, a set of CD spectra were recorded for mixtures of DNA (5 μM) with Dst (0–20 μM) at 13 (in a few cases, 12) different concentrations. The CD spectra were analyzed by singular value decomposition (SVD) to find significant spectral components (basis spectra) that contribute to the spectra [27,28]. For every DNA duplex examined here, the SVD analysis showed that three basis

spectra were required and enough to reproduce the observed CD spectra. If the CD spectrum observed for the i-th Dst–DNA mixture is denoted as $\boldsymbol{d}_i$ ($i=1$–13), then each $\boldsymbol{d}_i$ is expressed as a linear combination of the three basis spectra ($\boldsymbol{b}_j$, $j=1$–3) obtained by the SVD analysis:

$$\boldsymbol{d}_i = c_{i,1}\boldsymbol{b}_1 + c_{i,2}\boldsymbol{b}_2 + c_{i,3}\boldsymbol{b}_3 \quad (4)$$

where the coefficients $c_{i,j}$ are determined in the process of SVD of the experimental CD spectra.

Although Dst in free solution is optically inactive without giving any CD signals, its binding to chiral DNA duplexes can induce CD signals [29]. Accordingly, the appearance of three components in the CD spectra is consistent with the binding model (Eq. (1)) involving three optically active species, free DNA, Dst·DNA, and Dst_2·DNA. The spectra of the three molecular species $\boldsymbol{s}_k$ ($k=1$–3 for free DNA, Dst·DNA, and Dst_2·DNA) may also be expressed as a linear combination of $\boldsymbol{b}_j$ using unknown coefficients $f_{k,j}$ ($k=1$–3, $j=1$–3):

$$\boldsymbol{s}_k = f_{k,1}\boldsymbol{b}_1 + f_{k,2}\boldsymbol{b}_2 + f_{k,3}\boldsymbol{b}_3 \quad (5)$$

Furthermore, the observed spectrum $\boldsymbol{d}_i$ must be expressed as a linear combination of $\boldsymbol{s}_k$:

$$\boldsymbol{d}_i = [\mathrm{DNA}]_i\boldsymbol{s}_1 + [\mathrm{Dst{\cdot}DNA}]_i\boldsymbol{s}_2 + [\mathrm{Dst_2{\cdot}DNA}]_i\boldsymbol{s}_3 \quad (6)$$

where $[\mathrm{DNA}]_i$, $[\mathrm{Dst{\cdot}DNA}]_i$, and $[\mathrm{Dst_2{\cdot}DNA}]_i$ are the concentrations of the corresponding molecular species in the i-th mixture solution. Combining Eqs. (4)–(6), the following equation is obtained:

$$c_{i,j} = [\mathrm{DNA}]_i f_{1,j} + [\mathrm{Dst{\cdot}DNA}]_i f_{2,j} + [\mathrm{Dst_2{\cdot}DNA}]_i f_{3,j} \quad (7)$$

The values of $[\mathrm{DNA}]_i$, $[\mathrm{Dst{\cdot}DNA}]_i$, and $[\mathrm{Dst_2{\cdot}DNA}]_i$ ($i=1$–13) are expressed by using two unknown parameters K_1 and K_2 together with the total concentrations of Dst and DNA in the mixture (Eqs. (2) and (3)). Accordingly, the number of unknown parameters on the right side of Eq. (7) is 11 [K_1, K_2, and 9 $f_{k,j}$ ($k=1$–3, $j=1$–3)], while the number of experimental quantities on the left side is 39 [$c_{i,j}$ ($i=1$–13, $j=1$–3)]. Thus, the 11 unknown parameters can be determined to best reproduce the 39 experimental quantities by least-squares calculations. Once the most probable values of the unknown parameters are obtained, the spectra of three molecular species ($\boldsymbol{s}_k$) and their concentrations ($[\mathrm{DNA}]_i$, $[\mathrm{Dst{\cdot}DNA}]_i$, and $[\mathrm{Dst_2{\cdot}DNA}]_i$) in individual Dst–DNA mixtures are calculated by using Eqs. (2), (3), and (5). Following the procedures described above, CD spectra of Dst–DNA mixtures were analyzed on a personal computer with a computer program written in Visual C++ and Visual Basic.

3. Results

3.1. Binding of Dst to ATAAT

Boger et al. have shown that Dst most prefers the ATAAT sequence among the possible 512 pentamer sequences by using a fluorescent intercalator displacement method [24]. We have first examined the binding mode of Dst to a double-stranded DNA oligomer containing the most preferred sequence, d(5′-GGCATAATCGC-3′)·d(5′-GCGATTATGCC-3′), which is named ATAAT (Fig. 2). Fig. 3 shows CD spectra of mixtures of Dst (0–20 μM) and ATAAT (5 μM). The arrows in the figure indicate the directions of spectral changes associated with the increase of Dst concentration from 0 to 20 μM. The set of CD spectra in Fig. 3 exhibits an isodichroic point at 243 nm, which might be regarded as an indicator of a two component system. However, close examination of the spectra reveals that the spectral change is not monophasic but biphasic. The intensity around 280 nm first decreases and then increases with increase of the Dst concentration. A band around 325 nm increases in intensity first without change in peak position and then with a peak shift toward the longer wavelength side. The biphasic spectral changes suggest the presence of three components in the system as confirmed by the SVD analysis.

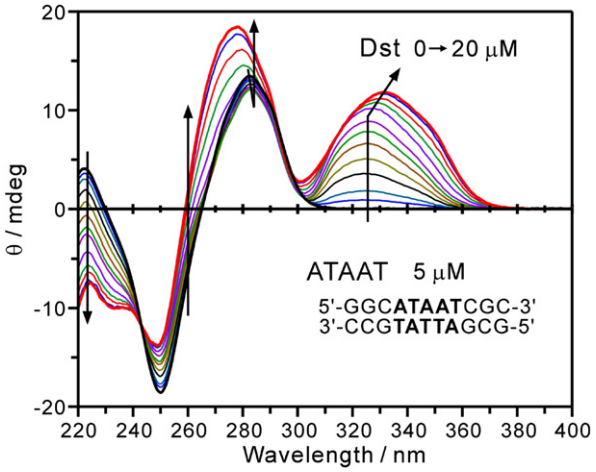

Fig. 3. CD spectra of mixtures of Dst (0–20 μM) and ATAAT (5 μM). The arrows indicate the spectral changes associated with the increase of Dst concentration from 0 to 20 μM.

Analysis of the CD spectra in Fig. 3 by the method described in Section 2.3 gave the most probable values of K_1 ($6.62\pm3.18\times10^6\ \mathrm{M}^{-1}$) and K_2 ($0.23\pm0.07\times10^6\ \mathrm{M}^{-1}$) together with those of 9 coefficients $f_{k,j}$. Fig. 4A shows the spectra ($\boldsymbol{s}_k$) of free DNA, Dst·DNA, and Dst_2·DNA (DNA = ATAAT) calculated from $f_{k,j}$ and the basis

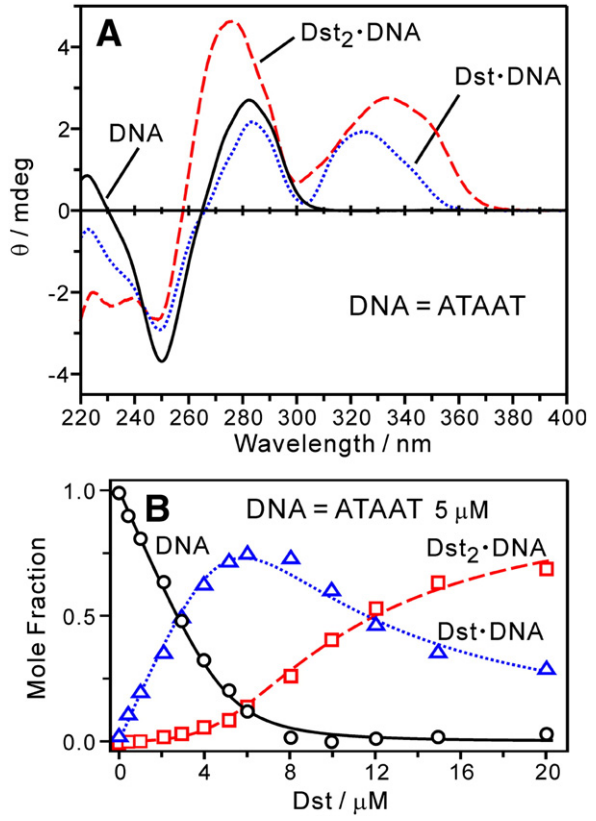

Fig. 4. (A) CD spectra of free DNA (ATAAT), Dst·DNA, and Dst_2·DNA extracted from the experimental CD spectra in Fig. 3 by the SVD-based equilibrium binding analysis. The intensity of each spectrum corresponds to that at a concentration of 1 μM. (B) Plot of the mole fractions of free DNA, Dst·DNA, and Dst_2·DNA against the total Dst concentration. The data points were obtained from the experimental CD spectra and the curves were calculated by using the binding constants K_1 and K_2 obtained by the equilibrium binding analysis.

spectra ($\boldsymbol{b}_j$) by using Eq. (5). The spectrum of free DNA well corresponds to that in the absence of Dst (Fig. 2). (The intensity in Fig. 4A is reduced to one-fifth of that in Fig. 2 because the spectra in Fig. 4A are calculated for a concentration of 1 μM). In the spectra of Dst·DNA and Dst_2·DNA, the broad signal in the 300–380 nm region is assigned to an induced CD signal of Dst [26,29], while the signals below 300 nm are due to an overlap of induced CD of Dst and intrinsic CD of DNA. The induced CD signals of Dst are ascribed, at least partly, to a slight twist of the *N*-methylpyrrole carboxamide backbone of Dst caused by the interaction with DNA [12,30].

Fig. 4B shows the mole fractions of free DNA, Dst·DNA, and Dst_2·DNA as a function of the total Dst concentration in the Dst–DNA (ATAAT) mixture. The data points marked with a circle (DNA), triangle (Dst·DNA), or square (Dst_2·DNA) are obtained from the observed CD spectra (Eq. (6)), while the three binding curves are calculated by using the K_1 and K_2 values obtained by the equilibrium binding analysis (Eqs. (2) and (3)). The close agreement between the experimental data points and the theoretical curves ensures that the Dst–DNA binding is well described by the equilibrium binding model described in Eq. (1). The plot in Fig. 4B indicates that the 1:1 complex is dominant in the presence of equimolar Dst and DNA, while the dominance of the 2:1 complex is achieved at Dst/DNA molar ratios above 2.5 (Dst concentration > 12.5 μM). Probably, the minor groove of the ATAAT duplex, to which Dst is expected to bind (Fig. 1B and C) [11–18], has a width and a depth appropriate for tight binding of a single Dst molecule but not enough deformability to readily accept two Dst molecules stacked side-by-side.

3.2. Substitution of the terminal residues of ATAAT

Substitution of either or both of the terminal residues of ATAAT was reported to significantly decrease the affinity of DNA for Dst [24]. We have examined the effect of the terminal residue substitution by CD spectroscopy using ATAAA, TTAAT, and TTAAA, in which the underlined residues are substituted for the corresponding residues of ATAAT (see Fig. 2). The K_1 and K_2 values obtained for the varied pentamer sequences are compared with those of the original sequence ATAAT in Table 1. The mole fractions of free DNA (x_0), Dst·DNA (x_1), and Dst_2·DNA (x_2) in an equimolar (5 μM) mixture of Dst and DNA are also listed in the table. The K_1 value decreases in the order of ATAAT, ATAAA, TTAAT, and TTAAA, whereas the K_2 value increases in the same order. The x_0 value, an indicator of the weakness of affinity, also increases in the same order, being consistent with the previous result of fluorescent intercalator displacement assay [24].

For the lowest-affinity pentamer TTAAA in Table 1, K_2 is much larger than K_1, suggesting a strong preference for 2:1 binding. The predominance of the 2:1 binding mode in the Dst–TTAAA system is seen more clearly in the binding curve shown in Fig. 5B. The 2:1 complex is more populated than the 1:1 complex except at very low Dst concentrations (<2 μM). Another characteristic of TTAAA is that the spectrum of the 2:1 complex (Dst_2·DNA in Fig. 5A) is significantly different from that of ATAAT (Fig. 4A), though the spectra of free DNA and the 1:1 complex are similar between the two A/T stretches. In the 2:1 complex of ATAAT, the positive CD band around 270 nm is much stronger than the band at 330 nm ($I_{270} > I_{330}$, Fig. 4A), whereas the peak intensities of two bands at 270 and 330 nm are comparable in the 2:1 complex of TTAAA ($I_{270} \approx I_{330}$, Fig. 5A). This observation suggests a significant difference in structure between the 2:1 complexes of ATAAT and TTAAA. Since the 2:1 complex is more stable for TTAAA than for ATAAT as judged from the binding constants, TTAAA may have an increased deformability of the minor groove to better accommodate two Dst molecules. The terminal residues of pentameric A/T stretches such as ATAAT and TTAAA are likely to play a role in determining the minor groove deformability, which is reflected in the stability of the 2:1 complex and in the preference for 1:1 or 2:1 binding.

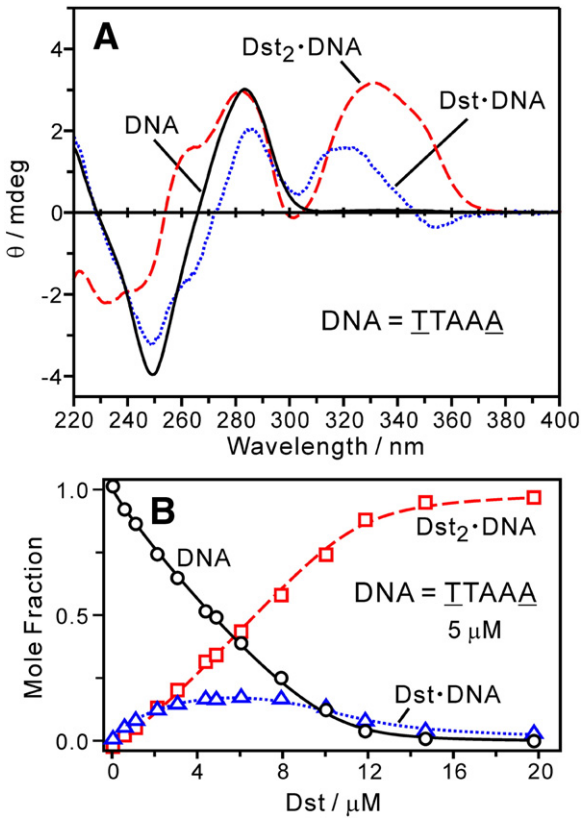

Fig. 5. (A) CD spectra of free DNA (TTAAA), Dst·DNA, and Dst_2·DNA. (B) Plot of the mole fractions of free DNA, Dst·DNA, and Dst_2·DNA against the total Dst concentration. For more details, see the caption to Fig. 4.

Table 1
Binding constants (K_1 and K_2) of Dst to pentameric A/T stretches and mole fractions of DNA components in an equimolar mixture.

DNA[a]	$K_1/10^6\ M^{-1}$	$K_2/10^6\ M^{-1}$	x_0[b]	x_1[b]	x_2[b]
ATAAT	6.62 ± 3.18	0.23 ± 0.07	0.20	0.71	0.09
ATAAA	3.29 ± 1.08	0.48 ± 0.13	0.28	0.56	0.16
TTAAT	1.82 ± 0.56	1.46 ± 0.47	0.37	0.36	0.27
TTAAA	0.64 ± 0.27	3.69 ± 1.65	0.47	0.17	0.36

[a] For the full base sequence, see Fig. 2.
[b] x_0, x_1, and x_2 stand for the mole fractions of free DNA, Dst·DNA, and Dst_2·DNA, respectively, calculated from K_1 and K_2 for an equimolar (5 μM) mixture of Dst and DNA.

3.3. Addition of A/T residues to ATAAT

As shown above, the mode of Dst binding strongly depends on the terminal residues of pentameric A/T stretches. To further examine the terminal residue effect, we prepared longer A/T stretches by adding two A/T residues to the core ATAAT. The binding constants (K_1 and K_2) obtained for such heptameric A/T stretches are summarized in Table 2. Mole fractions of the DNA components in an equimolar (5 μM) Dst–DNA mixture (x_0, x_1, and x_2) are also compared in the table. From the relative magnitude of K_1 and K_2 or the values of x_0, x_1, and x_2, the heptameric A/T stretches examined here are classified into two groups. The first group comprises AATAATT and TATAATT. The K_1 values of these A/T stretches are much larger than the K_2 values with $x_1 \gg x_2$ as was seen in the case of ATAAT (Table 1), implying that the added residues (double underlined) do not significantly affect the Dst binding.

In the second group consisting of AATAATA, TATAATA, and ATAATAT, K_1 is much smaller than K_2, favoring the 2:1 binding mode and exhibiting high x_0 values (low affinities) (Table 2). The second

Table 2
Binding constants (K_1 and K_2) of Dst to heptameric A/T stretches and mole fractions of DNA components in an equimolar mixture.

DNA[a]	$K_1/10^6\ M^{-1}$	$K_2/10^6\ M^{-1}$	x_0[b]	x_1[b]	x_2[b]
AATAATA	0.80 ± 0.46	2.44 ± 1.50	0.45	0.22	0.33
AATAATT	6.25 ± 4.03	0.35 ± 0.17	0.21	0.67	0.12
TATAATA[c]	0.33 ± 0.38	15.2 ± 18.3	0.51	0.07	0.42
TATAATT	2.35 ± 1.20	0.07 ± 0.04	0.27	0.68	0.05
ATAATAT[c]	0.30 ± 0.30	4.79 ± 5.00	0.52	0.11	0.37

[a] For the full base sequence, see Fig. 2.
[b] x_0, x_1, and x_2 stand for the mole fractions of free DNA, Dst·DNA, and Dst_2·DNA, respectively, calculated from K_1 and K_2 for an equimolar (5 μM) mixture of Dst and DNA.
[c] The large standard errors for K_1 and K_2 arise from a very small population of the 1:1 complex. If we neglect the 1:1 complex and assume a concerted binding of two Dst molecules, the binding constant K becomes $4.35 \pm 0.85 \times 10^{11}\ M^{-2}$ for TATAATA and $4.70 \pm 1.04 \times 10^{11}\ M^{-2}$ for ATAATAT.

group is characterized by the presence of a common base sequence of ATAATA, which is extended by only one additional A residue at the 3′-end of ATAAT. The last TpA step in ATAATA may play an important role in increasing the deformability of the minor groove for better accommodation of two Dst molecules. A combined NMR and molecular dynamics study has suggested that the last TpA step in an analogous A/T stretch (AATTA) increases the deformability at the TpA step allowing a widening of the minor groove [31]. This may also be the case for ATAATA and the increased deformability of ATAATA may be advantageous for 2:1 binding but not for 1:1 binding. Possibly, a tight 1:1 binding requires the minor groove with a limited deformability, whereas a stable 2:1 binding requires a loose and largely deformable minor groove.

The spectra of DNA, Dst·DNA, and Dst_2·DNA for the heptameric A/T stretches of the first group are close to those for the pentamer ATAAT, sharing a common intensity pattern of $I_{270} > I_{330}$ in the 2:1 complex. This is reasonable because the members of the first group and ATAAT all favor the 1:1 binding. It is likely that Dst binds to the ATAAT region within the pentameric A/T stretches of the first group and the A/T bases added to the 5′- and 3′-ends are not involved in the Dst binding as suggested above from the binding constants.

The second group of the pentameric A/T stretches, on the other hand, is not a simple extension of ATAAT. Fig. 6 demonstrates the binding curves and the spectra of DNA, Dst·DNA, and Dst_2·DNA for AATAATA that belongs to the second group. In the 2:1 complex (Dst_2·DNA), the CD bands around 270 and 330 nm have a comparable intensities ($I_{270} \approx I_{330}$, Fig. 6A), which is clearly different from that for ATAAT preferring 1:1 binding ($I_{270} > I_{330}$, Fig. 4A), but rather similar in shape to that for TTAAA preferring 2:1 binding ($I_{270} \approx I_{330}$, Fig. 5A). A major noticeable difference between AATAATA and TTAAA is that both CD bands around 270 and 330 nm are amplified for AATAATA by about 30% compared to ATAAT. The intensity increase suggests a stronger interaction of non-chiral Dst with chiral DNA in the 2:1 complex of AATAATA. Analogous CD spectra of Dst_2·DNA were also observed for the other members of the second group (data not shown). The A/T stretches that prefer 2:1 binding are likely to share a common type of Dst–DNA interaction in the 2:1 complex, which is different from that in the 2:1 complexes of the A/T stretches preferring 1:1 binding. The type of Dst–DNA 2:1 interaction as well as the binding mode preference is sensitive to the terminal A/T residues of the Dst binding region.

3.4. Addition of G/C bases to ATAAT

To study whether the terminal residue effect on the Dst binding is specific to the A and T nucleotides, we have examined the Dst binding to CATAATC and GATAATC, in which G or C is added to both ends of ATAAT (Fig. 2). The binding constants obtained are $K_1 = 5.85 \pm 3.29 \times 10^{-6}\ M^{-1}$ and $K_2 = 0.25 \pm 0.10 \times 10^{-6}\ M^{-1}$ for CATAATC and $K_1 = 6.79 \pm 4.81 \times 10^{-6}\ M^{-1}$ and $K_2 = 0.17 \pm 0.08 \times 10^{-6}\ M^{-1}$ for GATAATC. These binding constants are very close to those of ATAAT (Table 1), indicating that the addition of G/C residues does not affect the binding affinity nor the binding mode preference of the A/T stretch ATAAT. The terminal residue effect on the Dst binding is specifically induced by the A and T nucleotides.

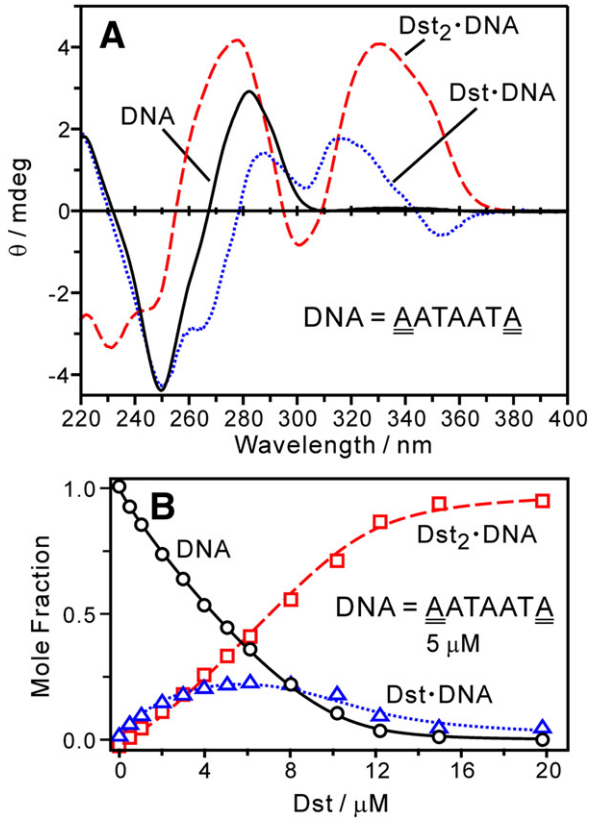

Fig. 6. (A) CD spectra of free DNA (AATAATA), Dst·DNA, and Dst_2·DNA. (B) Plot of the mole fractions of free DNA, Dst·DNA, and Dst_2·DNA against the total Dst concentration. For more details, see the caption to Fig. 4.

4. Discussion

The binding constants listed in Tables 1 and 2 show that the A/T stretches examined here prefer either 1:1 binding with $K_1 \gg K_2$ or 2:1 binding with $K_2 \gg K_1$. An exception is TTAAT, which has comparable K_1 and K_2 values without exhibiting any binding mode preference (Table 1). If we define the overall affinity of DNA for Dst by $1 - x_0$ (or $x_1 + x_2$), the overall affinity is in the following order: ATAAT ≈ AATAATT > TATAATT ≈ ATAAA ≫ TTAAT ≫ AATAATA ≈ TTAAA > TATAATA ≈ ATAATAT (see Tables 1 and 2). The large decrease of affinity in going from ATAAA to AATAAT A via TTAAT is associated with a change of the preferred binding mode from 1:1 to 2:1. The overall affinity of an A/T stretch to Dst is thus correlated with its preference for 1:1 binding over 2:1 binding. The preference depends both on the number and order of A/T residues in the stretch, and there seems no simple rule that governs the preference.

A foot printing study on tetrameric A/T stretches has proposed that TpA steps decrease the affinity for Dst [9]. However, this proposal cannot be generalized to include the pentameric and heptameric A/T stretches studied here. For example, all of ATAAT, ATAAA, TTAAT, and TTAAA contain a single TpA step, but the affinity for Dst largely decreases in that order as shown in Table 1. Furthermore, TATAATT and ATAAT AT, both having two TpA steps, exhibit completely different affinities (Table 2). Accordingly, the affinity for Dst is not simply related to the number of TpA steps in the sequence.

The position of the TpA step in the sequence may, however, be correlated with the binding affinity as far as the heptameric A/T stretches are concerned. AATAATA, TATAATA, and ATAATAT, all preferring the 2:1 binding and exhibiting low affinities, have a TpA step in the vicinity of the 3′-end, suggesting that such a TpA step allows a widening of the minor groove to accommodate two Dst molecules [31]. In the crystal structure of a 2:1 Dst–d(GTATATAC)$_2$ complex [18], the ribose ring of the 3′-terminal A residue is located near the propylamidinium tail of a Dst molecule. Possibly, a widening of the minor groove near the 3′-end is required for stably accommodating the propylamidinium tail of Dst in the 2:1 complex and a TpA step at or near the 3′-end plays a role in increasing the deformability of the minor groove to allow such widening. In contrast to the heptameric A/T stretches discussed above, the binding affinity of the pentameric A/T stretches seems to be dependent on both terminal residues (Table 1).

As described in Sections 3.2 and 3.3, the intensity of the positive CD band at 270 nm is larger than that at 330 nm ($I_{270}>I_{330}$) in the 2:1 complexes of the A/T stretches preferring 1:1 binding, whereas the intensities of both bands are comparable ($I_{270}\approx I_{330}$) in the 2:1 complexes of the A/T stretches preferring 2:1 binding (Figs. 4–6). Ivanov et al. investigated CD spectra of Dst bound to the A and B forms of a duplex containing a seven repeat of A (or T) under the conditions of a large excess of Dst, thereby 2:1 complexes being predominant [32]. The intensity patterns of the 270- and 330-nm CD bands in the Dst complexes with the A and B forms were $I_{270}>I_{330}$ and $I_{270}\approx I_{330}$, respectively, which are similar to those of the 2:1 complexes of the 1:1- and 2:1-preferring A/T stretches studied here. Since the minor groove in the A form of DNA is wider and shallower than that in the B form [33], it is likely that two Dst molecules are weakly bound in a wide but shallow minor groove of the 1:1-preferring A/T stretches, while they are strongly and deeply bound in the minor groove of 2:1-preferring A/T stretches. The depth of binding may be important in the stability of the 2:1 complex. Although the detailed mechanism of the terminal residue effect is not clear at present, it is evident that the terminal residues of the Dst binding region can significantly affect both the affinity and mode of Dst binding.

5. Conclusions

The A/T stretches that prefer 1:1 binding have higher affinities than the A/T stretches that prefer 2:1 binding. Although the former A/T stretches can bind two Dst molecules in their minor grooves, the Dst–DNA interaction in such a 2:1 complex is different from that in the 2:1 complex of the latter A/T stretches. Each type of DNA is likely to have a structure and a deformability particularly suited to the 1:1 or 2:1 binding. The terminal residues of A/T stretches composed of five-to-seven residues affect the binding affinity and the binding mode preference by changing the structure and deformability of the minor groove. The SVD-based equilibrium binding analysis is useful in revealing both the binding affinity and the binding mode in a single set of experiment as demonstrated here, and it may be applied to other drug–DNA interactions.

References

[1] F. Arcamone, S. Penco, P. Orezzi, V. Nicolella, A. Pirelli, Structure and synthesis of Distamycin A, Nature 203 (1964) 1064–1065.
[2] B. Puschendorf, H. Grunicke, Effect of distamycin A on the template activity of DNA in a DNA polymerase system, FEBS Lett. 4 (1969) 355–357.
[3] C. Zimmer, Effects of antibiotics netropsin and distamycin A on the structure of nucleic acids, Prog. Nucleic Acid Res. Mol. Biol. 15 (1975) 285–318.
[4] C. Zimmer, U. Wähnert, DNA-binding ligands: specificity of the interaction and their use as tools in biophysical, biochemical and biological investigations of the genetic material, Prog. Biophys. Mol. Biol. 47 (1986) 31–112.
[5] S.M. Nelson, L.R. Ferguson, W.A. Denny, Non-covalent ligand/DNA interactions: minor groove binding agents, Mutation Res. 623 (2007) 24–40.
[6] M.W. Van Dyke, R.P. Hertzberg, P.B. Dervan, Map of distamycin, netropsin, and actinomycin binding sites on heterogeneous DNA: DNA cleavage-inhibition patterns with methidiumpropyl-DTA·Fe(II), Proc. Natl. Acad. Sci. USA 79 (1982) 5470–5474.
[7] E.L. Fish, M.J. Lane, J.N. Vournakis, Determination of equilibrium binding affinity of distamycin and netropsin to the synthetic deoxyoligonucleotide sequence d(GGTATACC)$_2$ by quantitative DNase I footprinting, Biochemistry 27 (1988) 6026–6032.
[8] M.E.A. Churchill, J.J. Hayes, T.D. Tullius, Detection of drug binding to DNA by hydroxyl radical footprinting. Relationship of distamycin binding sites to DNA structure and positioned nucleosomes on 5S RNA genes of *xenopus*, Biochemistry 29 (1990) 6043–6050.
[9] A. Abu-Daya, P.M. Brown, K.R. Fox, DNA sequence preferences of several AT-selective minor groove binding ligands, Nucleic Acids Res. 23 (1995) 3385–3392.
[10] A. Abu-Daya, K.R. Fox, Interaction of minor groove binding ligands with long AT tracts, Nucleic Acids Res. 25 (1995) 4962–4969.
[11] A.J. Hampshire, K.R. Fox, The effects of local DNA sequence on the interaction of ligands with their preferred binding sites, Biochimie 90 (2008) 988–998.
[12] M. Coll, C.A. Frederick, A.H.J. Wang, A. Rich, A bifurcated hydrogen-bonded conformation in the d(AT) base pairs of the DNA dodecamer d(CGCAAATTTGCG) and its complex with distamycin, Proc. Natl. Acad. Sci. USA 84 (1987) 8385–8389.
[13] K. Uytterhoeven, J. Sponer, L. Van Meervelt, Two 1:1 binding modes for distamycin in the minor groove of d(GGCCAATTGG), Eur. J. Biochem. 269 (2002) 2868–2877.
[14] J.G. Pelton, D.E. Wemmer, Structural characterization of a 2:1 distamycin d (CGCAAATTGGC) complex by two-dimensional NMR, Proc. Natl. Acad. Sci. USA 86 (1989) 5723–5727.
[15] J.G. Pelton, D.E. Wemmer, Binding modes of distamycin a with d(CGCAAATTTGCG)$_2$ determined by two-dimensional NMR, J. Am. Chem. Soc. 112 (1990) 1393–1399.
[16] P. Fagan, D.E. Wemmer, Cooperative binding of distamycin-A to DNA in the 2 1 mode, J. Am. Chem. Soc. 114 (1992) 1080–1081.
[17] X. Chen, B. Ramakrishnan, M. Sundaralingam, Crystal structures of the side-by-side binding of distamycin to AT-containing DNA octamers d(ICITACIC) and d (ICATATIC), J. Mol. Biol. 267 (1997) 1157–1170.
[18] S.N. Mitra, M.C. Wahl, M. Sundaralingam, Structure of the side-by-side binding of distamycin to d(GTATATAC)$_2$, Acta Cryst. D55 (1999) 602–609.
[19] G.L. Olsen, E.A. Louie, G.P. Drobny, S.T. Sigurdsson, Determination of DNA minor groove width in distamycin–DNA complexes by solid-state NMR, Nucleic Acids Res. 31 (2003) (2003) 5084–5089.
[20] T.J. Dwyer, B.H. Geierstanger, J.G. Pelton, D.E. Wemmer, Interaction of minor groove ligands to an AAATT/AATTT site: correlation of thermodynamic characterization and solution structure, Biochemistry 34 (1995) 2937–2945.
[21] F.-M. Chen, F. Sha, Circular dichroic and kinetic differentiation of DNA binding modes of distamycin, Biochemistry 37 (1998) 11143–11151.
[22] J. Lah, G. Vesnaver, Binding of distamycin A and netropsin to the 12mer DNA duplexes containing mixed ATAGC sequences with at most five or three successive AT base pairs, Biochemistry 39 (2000) 9317–9326.
[23] J. Lah, G. Vesnaver, Energetic diversity of DNA minor-groove recognition by small molecules displayed through some model ligand–DNA systems, J. Mol. Biol. 342 (2004) 73–89.
[24] D.L. Boger, B.E. Fink, S.R. Brunette, W.C. Tse, M.P. Hedrick, A simple, high-resolution method for establishing DNA binding affinity and sequence selectivity, J. Am. Chem. Soc. 123 (2001) 5878–5891.
[25] J.D. Puglisi, I. Tinoco Jr., Absorbance melting curves of RNA, Methods Enzymol. 180 (1989) 304–325.
[26] G. Luck, C. Zimmer, K.-E. Reinert, F. Arcamone, Specific interactions of distamycin A and its analogs with (A·T) rich and (G·C) rich duplex regions of DNA and deoxypolynucleotides, Nucleic Acids Res. 4 (1977) 2655–2670.
[27] S.D. Frans, J.M. Harris, Least squares singular value decomposition for the resolution of p*K*'s and spectra from organic acid/base mixtures, Anal. Chem. 57 (1985) 1718–1721.
[28] R.W. Hendler, R.I. Shrager, Deconvolutions based on singular value decomposition and the pseudoinverse: a guide for beginners, J. Biochem. Biophys. Methods 28 (1994) 1–33.
[29] C. Zimmer, G. Luck, H. Thrum, C. Pitra, Binding of analogues of the antibiotics distamycin A and netropsin to native DNA, Eur. J. Biochem. 26 (1972) 81–89.
[30] D.S. Lu, Y. Nonaka, M. Tsuboi, K. Nakamoto, Molecular distortion of distamycin on binding to DNA as revealed by Raman spectroscopy, J. Raman Spectrosc. 21 (1990) 321–326.
[31] C.E. Bostock-Smith, C.A. Laughton, M.S. Searle, Solution structure and dynamics of the A–T tract DNA decamer duplex d(GGTAATTACC)$_2$: implications for recognition by minor groove binding drugs, Biochem. J. 342 (1999) 125–132.
[32] V.I. Ivanov, L.E. Minchenkova, G. Burckhardt, E. Birch-hirschfeld, H. Fritzsche, C. Zimmer, The detection of B-form/A-form junction in a deoxyribonucleotide duplex, Biophys. J. 71 (1996) 3344–3349.
[33] W. Saenger, Principles of Nucleic Acid Structure, Springer-Verlag, New York, 1984.